BSc report APPLIED MATHEMATICS

“Modelling cloggings in a geothermal reservoir”

EBRU ATIS

Delft University of Technology

Delft, Netherlands
July, 2020

Supervisors

Dr. B.J. Meulenbroek

Committee members

Prof. dr. ir. A.W. Heemink Dr. J.G. Spandaw

Contents

Abstract

Due to an increase of precipitation reactions in water by temperature changes, cloggings can occur in a geothermal doublet. A consequence of the cloggings is that the process of generating geothermal energy becomes inefficient eventually. Our goal is to determine which minerals play an important role in the clogging process in each part of the geothermal doublet. First, we have divided the geothermal doublet into four tanks. Then we have derived a general model for a general chemical reaction. Afterwards, we have used this model for 5 kinds of mineralisation reactions. This led to first-order differential equations, which we have solved analytically or numerically with the Forward Euler method. Finally, we have concluded that the minerals barite, calcite, dolomite and goethite play an important role in the clogging process in tank 3 and tank 4.

1. Introduction

Fossil fuels (such as oil, gas and coal) are the world's main energy sources. However, these resources are limited. If we keep on using fossil fuels at our current rate, we will run out of fossil fuels over the coming decades. To keep up with the future energy demand, we will need alternative, renewable energy sources. For example, wind and solar energy are such alternatives. Since wind and sunlight are not always available, we will look for energy sources that are also reliable. In our report, we will focus on such a renewable and reliable energy source, namely geothermal energy.

First of all, what is geothermal energy? Due to radioactive decay within the Earth, heat is being produced. This internal heat is stored in the rocks and fluids beneath the Earth's surface. The energy generated from Earth's internal heat is called geothermal energy.

This geothermal energy can be extracted from the Earth's subsurface. The process of generating geothermal energy is illustrated in figure 1. Two wells are drilled into the Earth's subsurface at a certain depth such that the temperature of the water is approximately 80 ^{o}C. In volcanic regions (such as Iceland), this depth is approximately a few 100 meters. Our geothermal plant is in the Netherlands and here we need to drill approximately 2 km to achieve high temperature. The injector well injects the cold water into the geothermal reservoir and pumps it through the subsurface, where the cold water is heated by the hot environment, to the production well. Then the production well extracts the hot water and pumps it through a heat exchanger. This extracted heat can be used, for example, to generate electricity or to heat up buildings. Consequently, the cooled water is transferred to the injector well.

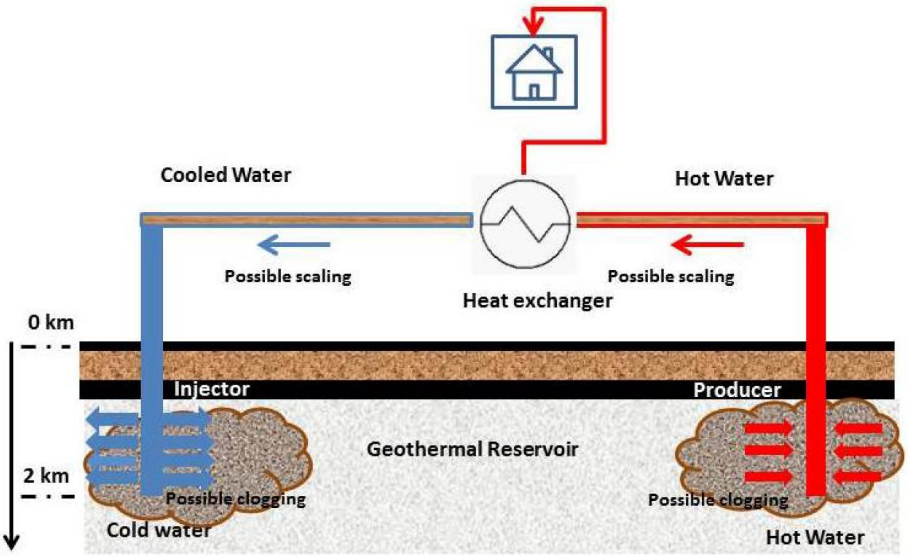

Figure 1: The process of generating geothermal energy.

The advantage of the above-mentioned process is that it is environmentally friendly since the CO_2 emission is low compared to fossil fuels. Also, note that we only circulate the fluid, which makes geothermal energy a renewable energy source. However, the pressure in the subsurface changes due to the pumping of water. This change can trigger earthquakes. But in our case, the pressure change remains approximately constant, so the chance of earthquakes is negligibly small.

The energy costs of a geothermal doublet (figure 1) consists of two kinds, namely:

- Drilling costs: the energy costs for implementing a geothermal doublet.
- Pumping costs: the energy costs for pumping.

The drilling costs are one-time costs and these are lower than the pumping costs. Therefore, we will focus on the pumping costs.

The location of a geothermal plant is chosen initially such that the gained energy is higher than the input energy. However, at some point we will need more pumping energy to keep the circulation ongoing due to possible 'cloggings'. Eventually, the pumping energy will exceed the amount of energy produced and generating geothermal energy will become an inefficient process.

Cloggings arise from precipitations of naturally dissolved minerals in water. The dissolution/precipitation reaction of these minerals are in equilibrium. Due to temperature changes, this equilibrium shifts. For example, when we inject the cold water into the subsurface, the temperature of the subsurface water decreases and some of the dissolved minerals in the water precipitate on the rock grains. As a result, the void spaces (pores) in the geothermal reservoir get clogged.

The aim of this project is to investigate which minerals play an important role in the clogging process in every segment of the reservoir. We will first divide the geothermal doublet into 4 tanks. Then we will build up a general model for a general chemical reaction. This we will do by deriving the rate equations for the reaction, which leads to first-order differential equations. Next, we will apply the general model to specific chemical reactions and we will solve the corresponding ODE's analytically or numerically. Eventually, we will investigate which chemical reactions play an important role in the clogging process in each tank.

The structure of the reports is as follows. In section 2, we will describe the general model. In section 3 and 4, we will use this model to determine the behaviour of some dissolved minerals in water. Finally, we will end the report with some conclusions in section 5 and an outlook in which we give some suggestions for making the process more efficient.

2. General model

In this section we will describe the overall model. We will first give a schematic overview of our geothermal reservoir in figure 1. In this figure, we have divided the reservoir into four parts. We will first estimate how long the water remains in each part of the four parts of the circulation. Then we will analyse which reaction are important in each part. This is done as follows. We assume that each tank behaves like a continuously stirred-tank reactor. This means that we assume that the tanks are perfectly mixed, i.e. the flow is constant and the contents are mixed uniformly. So in our model we neglect all spatial dependencies. This analysis tells us which reactions are important in each tank. Afterwards, we will derive a rate equation for a general chemical reaction. We will eventually use this derivation for specific reactions.

2.1. Schematic overview of a geothermal doublet

The process of generating geothermal energy described in the introduction, can be divided into 4 parts. A schematic diagram is given in figure 2. We will now describe the main processes in each tank and we will begin at the injection well. Via tank 3 (injection well), the cooled water is transported into tank 4 (geothermal reservoir). The first tank (producer well) has a temperature of $T = 80\ ^{o}$C, which remains constant for the whole life-span of the geothermal doublet. For the second tank, the temperature decreases from $T = 80\ ^{o}$C to $T = 20\ ^{o}$C due to the heat exchanger. Due to the temperature decrease in tank 2, precipitation of some minerals occurs. A filter is included in tank 2 such that the precipitated minerals are removed from the water.

Note that tank 3 includes also the wellbore region. The reason why we included the near wellbore region in tank 3 is that the cloggings have a more important influence here compared to the other tanks. For example, if there are cloggings in tank 4, then the water can flow around these cloggings to tank 1. But such alternative paths does not the water have near the wellbore region if this region is clogged.

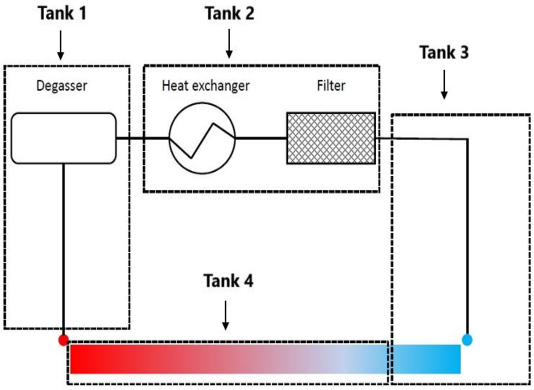

Figure 2: Schematic overview of generating geothermal energy.

In each tank, the water flows from one end to another for some time. We will call this residence time t_s. In our case, the flow rate is given as 300 m^3/hour for each tank. In table 1, we estimated t_s with the given flow rate and data for each tank.

Tank	Data	t_s
1	Tubing length and radius: 3000 m and 0.05 m Surface pipeline length and radius: 50 m and 0.127 m	5 min
2	Time in heat exchanger: 30 sec Time in filter: 30 sec	1 min
3	Surface pipeline length and radius: 50 m and 0.127 m Tubing length and radius: 3000 m and 0.05 m Wellbore height and radius: 30 m and 1 m	24 min
4	Distance between two wells: 1000 m Width and height: 500 m and 30 m	6 years

Table 1: The residence time t_s is estimated with the given data for each tank.

2.2. Derivation of a rate equation

We will now derive rate equations for a general reaction and we will apply this method in the next sections.

Rate equations relate the reaction rate with the concentrations or activities of the reactants. We will use molal concentrations, so the concentrations are measured in moles of solute per kg of solvent. The reason why we use molality instead molarity is that the molality is invariant to pressure change, which is not the case for molarity. For a species i, denote the molal concentration by m_i (mole/kgw) where the kgw stands for kg water.

Chemical reactions are often expressed in terms of activity a_i for a species i. The activities of solids and water are always equal to 1. First, we will relate the activity with the concentration. The activity is proportional to the concentration, that is

$$a_i = \frac{\gamma_i}{\gamma^o m^o} m_i \tag{1}$$

The γ_i is the dimensionless activity coefficient that depends on the temperature and the pressure of the solution. The γ^o is a coefficient and m^o is the standard molality. We set $\gamma^o = 1$ and $m^o = 1$ such that the units of equation (1) are on both sides equal.

Now, consider the following reversible chemical reaction:

$$\mathrm{n_1B + n_2C \underset{-}{\overset{+}{\rightleftharpoons}} n_3D} \tag{2}$$

where n_1, n_1 and n_3 are positive integers. We will only work with precipitation reactions that convert reactants to products in a single step, also known as elementary reactions. These reactions often occur on the interface of a solid. The area of this interface will be denoted by SA (m^2/kgw).

The reaction rates of reaction (2) are proportional to SA multiplied by the concentrations of reactants raised to an appropriate power. For instance, for the forward rate holds

$$R_+ \quad \sim SA \cdot a_B^{p_1} a_C^{p_2}$$

where p_1 and p_2 are the reaction orders. Since we work with elementary reactions, the reaction orders are usually equal to the stoichiometric coefficients of reaction (2). So for the forward rate we have $p_1 = n_1$ and $p_2 = n_2$. The reaction rate is also proportional to the reaction rate constant K, which includes the effects of variables such as temperature and pressure on the rate. The rate constant is determined experimentally. Thus, we have the following forward and backward rates of reaction (2):

$$\begin{cases} \text{forward rate} & = R_+ = SA \cdot K_+ a_B^{n_1} a_C^{n_2} \\ \text{backward rate} & = R_- = SA \cdot K_- a_D^{n_3} \end{cases} \tag{3}$$

where K_+ and K_- are the forward and backward reaction rate constants of (2), respectively. The surface area SA is artificial in our case since the reactions occur in water, but it is conventional to include it in the calculations.

Dependent on the reaction, one of the rate constants can be expressed by the Arrhenius equation:

$$K_{+/-} = A \cdot e^{\frac{-E_a}{RT}} \tag{4}$$

where R is the universal gas constant and T is the temperature in Kelvin. The A is called the pre-exponential factor, which denotes the frequency of collisions. The activation energy of the reaction is denoted by E_a. This is a measure of the minimum amount of energy required such that the reaction occurs. Both A and E_a are experimentally determined. Observe that the Arrhenius equation relates the rate constants with the temperature.

The other unknown rate constant can be determined by using the following relation:

$$K = \frac{K_-}{K_+} \tag{5}$$

The K in (5) is determined experimentally by fitting the following functional form:

$$^{10}\log(K) = A_1 + A_2 T + \frac{A_3}{T} + A_4 {}^{10}\log(T) + \frac{A_5}{T^2} + A_6 T^2 \tag{6}$$

where $A_1, A_2, ..., A_6$ are experimentally determined parameters and T is the temperature in Kelvin.

Finally, we can give the overall rate of appearance of substances B, C and D by combining the forward and backward rate as follows:

$$\begin{cases} \frac{dm_{\text{B}}}{dt} & = SA \cdot (K_- a_D^{n_3} - K_+ a_B^{n_1} a_C^{n_2}) \\ \frac{dm_{\text{C}}}{dt} & = SA \cdot (K_- a_D^{n_3} - K_+ a_B^{n_1} a_C^{n_2}) \\ \frac{dm_{\text{D}}}{dt} & = SA \cdot (K_+ a_B^{n_1} a_C^{n_2} - K_- a_D^{n_3}) \end{cases} \tag{7}$$

3. Rate equations of independent reactions

First, we will study two chemical reactions that are independent of each other. These are the reactions that form halite and barite, which are common dissolved minerals in water.

3.1. Halite

Consider the following reversible reaction of halite NaCl:

$$\mathrm{Na}^+ + \mathrm{Cl}^- \underset{-}{\overset{+}{\rightleftharpoons}} \mathrm{NaCl} \tag{8}$$

Let K_+ and K_- be the forward and backward rate constants of (8), respectively. Then we have

$$\begin{cases} \text{forward rate} & = R_+ = SA \cdot K_+ a_{\mathrm{Na}^+} a_{\mathrm{Cl}^-} \\ \text{backward rate} & = R_- = SA \cdot K_- a_{\mathrm{NaCl}} \end{cases} \tag{9}$$

The overall rate of appearance of Na^+ and Cl^- is the difference between R_- and R_+, i.e.

$$\begin{cases} \frac{dm_{\mathrm{Na}^+}}{dt} = SA \cdot K_- a_{\mathrm{NaCl}} - SA \cdot K_+ a_{\mathrm{Na}^+} a_{\mathrm{Cl}^-} \\ \frac{dm_{\mathrm{Cl}^-}}{dt} = SA \cdot K_- a_{\mathrm{NaCl}} - SA \cdot K_+ a_{\mathrm{Na}^+} a_{\mathrm{Cl}^-} \end{cases} \tag{10}$$

where t is the time. The equations in (10) contain both activity and concentration variables. Using equation (1), we can rewrite (10) as

$$\begin{cases} \frac{da_{\mathrm{Na}^+}}{dt} = \gamma_{\mathrm{Na}^+}(K_- a_{\mathrm{NaCl}} - K_+ a_{\mathrm{Na}^+} a_{\mathrm{Cl}^-})SA \\ \frac{da_{\mathrm{Cl}^-}}{dt} = \gamma_{\mathrm{Cl}^-}(K_- a_{\mathrm{NaCl}} - K_+ a_{\mathrm{Na}^+} a_{\mathrm{Cl}^-})SA \end{cases} \tag{11}$$

The activity coefficient γ depends on the temperature and the pressure of the solution. For our process, this coefficient is approximately equal to 1. Therefore, we will set $\gamma_{\mathrm{Na}^+} = \gamma_{\mathrm{Cl}^-} = 1$. Also, for our process we can assume that $SA = 1$. Substituting these values in (11) gives

$$\frac{da_{\mathrm{Na}^+}}{dt} = \frac{da_{\mathrm{Cl}^-}}{dt} \implies a_{\mathrm{Na}^+} + = a_{\mathrm{Cl}^-} + c \tag{12}$$

where c is some constant. This constant have to be zero due to charge conservation. Thus, we have $a_{\mathrm{Na}^+} = a_{\mathrm{Cl}^-}$. If we substitute this in (11), we get the following first-order differential equation:

$$\begin{cases} \frac{da}{dt} & = K_- - K_+ a^2 \\ a(t_0) & = a_0 \end{cases} \tag{13}$$

where a is the activity of sodium or chloride.

3.1.1. Equilibrium solutions

We will first determine the equilibrium points of (13). So

$$K_- - K_+ a_{eq}^2 = 0 \implies a_{eq} = \pm\sqrt{\frac{K_-}{K_+}} \tag{14}$$

Since $a > 0$ for all $t > 0$, follows that $a_{eq} = \sqrt{\frac{K_-}{K_+}}$ is the only equilibrium value of (13).

	a_{eq}
$T = 20\ ^o\mathrm{C}$	5.8320
$T = 80\ ^o\mathrm{C}$	6.2936

Table 2: Equilibrium values of equation (13) for sodium and chloride.

3.1.2. Analytical solutions

An exact solution of equation (13) can be obtained since it is separable, i.e. equation (13) can be written as

$$\frac{1}{K_- - K_+ a^2}\frac{da}{dt} = 1 \tag{15}$$

Consequently,

$$\int_{a_0}^{a} \frac{1}{K_- - K_+ s^2} ds = \int_{t_0}^{t} 1 ds \tag{16}$$

We will solve the left-hand side of (16) using partial fraction decomposition. Hence,

$$\begin{aligned}\int_{a_0}^{a} \frac{1}{K_- - K_+ s^2} ds &= \frac{1}{K_+}\int_{a_0}^{a} \frac{1}{(a_{eq} - s)(a_{eq} + s)} ds \\ &= \frac{1}{2a_{eq}K_+}\int_{a_0}^{a} \Big(\frac{1}{a_{eq} - s} + \frac{1}{a_{eq} + s}\Big) ds \\ &= \frac{1}{2a_{eq}K_+}[-\ln(|a_{eq} - s|) + \ln(a_{eq} + s)]_{s=a_0}^{a} = \frac{1}{2a_{eq}K_+}\Big[\ln\Big(\frac{a_{eq} + s}{|a_{eq} - s|}\Big)\Big]_{s=a_0}^{a}\end{aligned}$$

So rewriting equation (16) gives

$$\frac{1}{2a_{eq}K_+}\Big[\ln\Big(\frac{a_{eq} + a}{|a_{eq} - a|}\Big) - \ln\Big(\frac{a_{eq} + a_0}{|a_{eq} - a_0|}\Big)\Big] = t - t_0 \tag{17}$$

Hence, solving (17) for a gives the following analytical solution of (13):

$$a(t) = \begin{cases} a_{eq}\tanh(\sqrt{K_- K_+}(t + C)) & \text{if } a_{eq} > a_0 \\ a_{eq}\dfrac{1}{\tanh(\sqrt{K_- K_+}(t + C))} & \text{if } a_{eq} < a_0 \end{cases} \tag{18}$$

with

$$C = \frac{1}{2\sqrt{K_- K_+}}\ln\Big(\frac{a_{eq} + a_0}{|a_{eq} - a_0|}\Big) - t_0$$

Define K as equation (5). The backward rate constant of our process is given as

$$K_- = A_{\mathrm{NaCl}} \cdot e^{-\frac{E_a^{\mathrm{NaCl}}}{RT}} \tag{19}$$

where R is the universal gas constant, A_{NaCl} is the pre-exponential factor and E_a^{NaCl} is the activation energy, which is the minimum amount of energy needed for the dissolution of halite.

	NaCl
Arrhenius pre-exponential factor A [1/s]	12.3
Arrhenius activation energy E_a [J/mole]	7442

Table 3: Input for halite.

	NaCl
A_1	6.244800e+003
A_2	1.851478e+000
A_3	-2.624691e+005
A_4	-2.423205e+003
A_5	1.203027e+007
A_6	-6.099010e-004

Table 4: Parameters of K for halite.

In figure 3, the analytical solutions of (13) for sodium and chloride are plotted against time for $T = 20\ ^o$C. Here, we have taken as initial conditions the equilibrium solutions for $T = 80\ ^o$C. Also, in this figure the $y-$axis is scaled with

$$\frac{a(t) - a(t_0)}{a(t_0)} \tag{20}$$

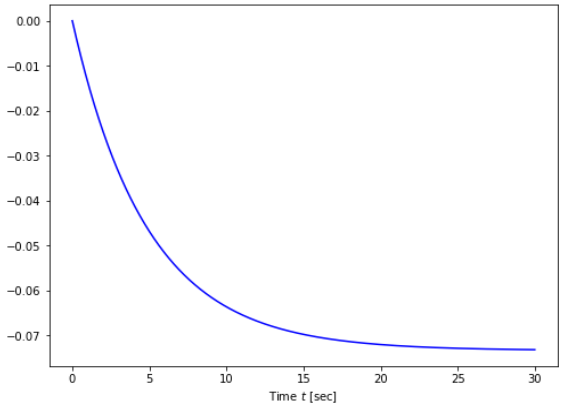

Figure 3: Activity of Na^+ and Cl^- versus time in seconds. The temperature decreases from $T = 80\ ^o$C to $T = 20\ ^o$C.

3.2. Barite

Consider the following reversible reaction of barite BaSO_4:

$$\text{Ba}^{2+} + \text{SO}_4{}^{2-} \overset{+}{\underset{-}{\rightleftharpoons}} \text{BaSO}_4 \tag{21}$$

Let K_+ and K_- be the forward and backward rate constants of (21), respectively. Then we have

$$\begin{cases} \text{forward rate} & = R_+ = SA \cdot K_+ a_{\text{Ba}^{2+}} a_{\text{SO}_4{}^{2-}} \\ \text{backward rate} & = R_- = SA \cdot K_- a_{\text{BaSO}_4} \end{cases} \tag{22}$$

The overall rate of appearance of Ba^{2+} and $\text{SO}_4{}^{2-}$ is the difference between R_- and R_+, i.e.

$$\begin{cases} \frac{dm_{\text{Ba}^{2+}}}{dt} = SA \cdot K_- a_{\text{BaSO}_4} - SA \cdot K_+ a_{\text{Ba}^{2+}} a_{\text{SO}_4{}^{2-}} \\ \frac{dm_{\text{SO}_4{}^{2-}}}{dt} = SA \cdot K_- a_{\text{BaSO}_4} - SA \cdot K_+ a_{\text{Ba}^{2+}} a_{\text{SO}_4{}^{2-}} \end{cases} \tag{23}$$

where t is the time. Using equation (1), we can write (23) as

$$\begin{cases} \frac{da_{\text{Ba}^{2+}}}{dt} = \gamma_{\text{Ba}^{2+}} (K_- a_{\text{BaSO}_4} - K_+ a_{\text{Ba}^{2+}} a_{\text{SO}_4{}^{2-}}) SA \\ \frac{da_{\text{SO}_4{}^{2-}}}{dt} = \gamma_{\text{SO}_4{}^{2-}} (K_- a_{\text{BaSO}_4} - K_+ a_{\text{Ba}^{2+}} a_{\text{SO}_4{}^{2-}}) SA \end{cases} \tag{24}$$

Since the activity coefficients and the surface area are approximately equal to 1 for our process, we will set $\gamma_{\text{Ba}^{2+}} = \gamma_{\text{SO}_4{}^{2-}} = 1$ and $SA = 1$. Then it follows that $a_{\text{Ba}^{2+}} = a_{\text{SO}_4{}^{2-}}$. Substituting these assumptions in (24), we get the first order differential equation described as in (13).

3.2.1. Analytical solutions

Let K be defined as equation (5). Since acidity affects rate constants, the backward rate constant of reaction (21) is given as

$$K_- = A_{\text{BaSO}_4} \cdot e^{-\frac{E_a^{\text{BaSO}_4}}{RT}} + A_{acid} \cdot e^{-\frac{E_a^{acid}}{RT}} a_{acid}^n \tag{25}$$

where the parameters are given in table 5 and 6. For our process, the pH remains constant due to the buffering capacity of water. Therefore, we can let $a_{acid} = 10^{-\text{pH}}$.

	BaSO_4	acid
Arrhenius pre-exponential factor A [1/s]	3.13e-003	3.09e-002
Arrhenius activation energy E_a [J/mole]	30780	30780

Table 5: Input for barite.

pH	6
n	0.22

Table 6: Parameters for barite.

	BaSO_4
A_1	3.630937e+003
A_2	1.218154e+000
A_3	-1.393850e+005
A_4	-1.437233e+003
A_5	5.362526e+006
A_6	-4.566328e-004

Table 7: Parameters of K for barite.

In figure 4, the analytical solutions of (13) for barium and sulfate are plotted against time for $T = 20\ ^o\text{C}$. Here, we have taken as initial conditions the equilibrium solutions for $T = 80\ ^o\text{C}$. Also, in this figure the $y-$axis is scaled as equation (20).

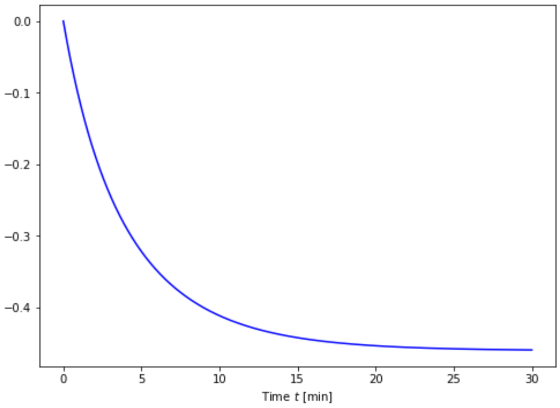

Figure 4: Activity of $\mathrm{Ba^{2+}}$ and $\mathrm{SO_4{}^{2-}}$ versus time in minutes. The temperature decreases from $T = 80\ ^o\mathrm{C}$ to $T = 20\ ^o\mathrm{C}$.

4. Rate equations of dependent reactions

We will now analyze dependent reactions, i.e. reactions that compete for the same ions. Consider the following reactions:

1. Calcite: $\mathrm{Ca^{2+} + HCO_3{}^- \underset{K^1_-}{\overset{K^1_+}{\rightleftharpoons}} CaCO_3 + H^+}$
2. Dolomite: $\mathrm{Ca^{2+} + Mg^{2+} + HCO_3{}^- \underset{K^2_-}{\overset{K^2_+}{\rightleftharpoons}} CaMg(CO_3)_2 + 2\,H^+}$
3. Goethite: $\mathrm{Fe^{3+} + 2\,H_2O \underset{K^3_-}{\overset{K^3_+}{\rightleftharpoons}} FeOOH + 3\,H^+}$

Let m_1, m_2, m_3, m_4 and m_5 be the molal concentrations of $\mathrm{Ca^{2+}}$, $\mathrm{HCO_3{}^-}$, $\mathrm{Mg^{2+}}$, $\mathrm{H^+}$ and $\mathrm{Fe^{3+}}$, respectively. Let SA^1, SA^2 and SA^3 be the reactive surface area of reaction (1), (2) and (3), respectively. Then for reaction (1) we have

$$\begin{cases} \text{forward rate} & = R^1_+ = SA^1 \cdot K^1_+ a_1 a_2 \\ \text{backward rate} & = R^1_- = SA^1 \cdot K^1_- a_{\mathrm{CaCO_3}} a_4 \end{cases} \tag{26}$$

For reaction (2) we have

$$\begin{cases} \text{forward rate} & = R^2_+ = SA^2 \cdot K^2_+ a_1 a_2 a_3 \\ \text{backward rate} & = R^2_- = SA^2 \cdot K^2_- a_{\mathrm{CaMg(CO_3)_2}} a_4^2 \end{cases} \tag{27}$$

and for reaction (3) we have

$$\begin{cases} \text{forward rate} & = R^3_+ = SA^3 \cdot K^3_+ a_5 a^2_{\mathrm{H_2O}} \\ \text{backward rate} & = R^3_- = SA^3 \cdot K^3_- a_{\mathrm{FeOOH}} a_4^3 \end{cases} \tag{28}$$

For reactions (1)-(3), we can assume that $SA^1 = SA^2 = SA^3 = 1$. Then we have the following overall rates:

$$\begin{cases} \frac{dm_1}{dt} &= K_-^1 a_4 - K_+^1 a_1 a_2 + K_-^2 a_4^2 - K_+^2 a_1 a_2 a_3 \\ \frac{dm_2}{dt} &= K_-^1 a_4 - K_+^1 a_1 a_2 + K_-^2 a_4^2 - K_+^2 a_1 a_2 a_3 \\ \frac{dm_3}{dt} &= K_-^2 a_4^2 - K_+^2 a_1 a_2 a_3 \\ \frac{dm_4}{dt} &= K_+^1 a_1 a_2 - K_-^1 a_4 + K_+^2 a_1 a_2 a_3 - K_-^2 a_4^2 + K_+^3 a_5 - K_-^3 a_4^3 \\ \frac{dm_5}{dt} &= K_-^3 a_4^3 - K_+^3 a_5 \end{cases} \tag{29}$$

Using equation (1), we can rewrite system (29) as

$$\begin{cases} \frac{da_1}{dt} &= \gamma_1 \cdot (K_-^1 a_4 - K_+^1 a_1 a_2 + K_-^2 a_4^2 - K_+^2 a_1 a_2 a_3) \\ \frac{da_2}{dt} &= \gamma_2 \cdot (K_-^1 a_4 - K_+^1 a_1 a_2 + K_-^2 a_4^2 - K_+^2 a_1 a_2 a_3) \\ \frac{da_3}{dt} &= \gamma_3 \cdot (K_-^2 a_4^2 - K_+^2 a_1 a_2 a_3) \\ \frac{da_4}{dt} &= \gamma_4 \cdot (K_+^1 a_1 a_2 - K_-^1 a_4 + K_+^2 a_1 a_2 a_3 - K_-^2 a_4^2 + K_+^3 a_5 - K_-^3 a_4^3) \\ \frac{da_5}{dt} &= \gamma_5 \cdot (K_-^3 a_4^3 - K_+^3 a_5) \end{cases} \tag{30}$$

Since the activity coefficient is approximately 1 for ionic solutions, we will set all activity coefficients equal to 1.

4.1. Equilibrium solutions

Let

$$K^1 = \frac{K_-^1}{K_+^1}, \quad K^2 = \frac{K_-^2}{K_+^2} \quad \text{and} \quad K^3 = \frac{K_-^3}{K_+^3} \tag{31}$$

To obtain the equilibrium points of system (30), it comes to solving the following equations:

$$\begin{cases} K_-^1 a_4 - K_+^1 a_1 a_2 + K_-^2 a_4^2 - K_+^2 a_1 a_2 a_3 &= 0 \\ K_-^2 a_4^2 - K_+^2 a_1 a_2 a_3 &= 0 \\ K_-^3 a_4^3 - K_+^3 a_5 &= 0 \end{cases} \tag{32}$$

For our problem, the reactions (1)-(3) are in steady state at time t_0. The pH is then known. Due to charge conservation, we have

$$a_1 + a_3 + a_4 = 5a_2 \tag{33}$$

Combining (32) and (33) gives the following equilibrium solutions:

$$\begin{cases} a_1^{eq} &= -\frac{1}{2}(a_3^{eq} + a_4^0) + \frac{5}{2}\sqrt{[\frac{1}{5}(a_3^{eq} + a_4^0)]^2 + \frac{4}{5}K^1 a_4^0} \\ a_2^{eq} &= \frac{1}{5}(a_1^{eq} + a_3^{eq} + a_4^0) \\ a_3^{eq} &= \frac{K^2}{K^1} a_4^0 \\ a_5^{eq} &= \frac{K_-^3}{K_+^3}(a_4^0)^3 \end{cases} \tag{34}$$

with $a_4^0 = 10^{-\text{pH}}$.

4.2. Numerical solutions

The value of K^1, K^2 and K^3 can be determined by using equation (5) and (6). The forward rates for reaction (1) and (2) are given by

$$\begin{aligned} K_+^{\mathrm{CaCO_3}} &= A_{\mathrm{CaCO_3}} \cdot e^{-\frac{E_a^{\mathrm{CaCO_3}}}{RT}} + A_{\mathrm{HCO_3}^-} \cdot e^{-\frac{E_a^{\mathrm{HCO_3}^-}}{RT}} a_2^n \\ K_+^{\mathrm{CaMg(CO_3)_2}} &= A_{\mathrm{CaMg(CO_3)_2}} \cdot e^{-\frac{E_a^{\mathrm{CaMg(CO_3)_2}}}{RT}} + A_{\mathrm{HCO_3}^-} \cdot e^{-\frac{E_a^{\mathrm{HCO_3}^-}}{RT}} a_2^n \end{aligned} \tag{35}$$

and the backward rate of reaction (3) is given by

$$K_-^{\mathrm{FeOOH}} = A_{\mathrm{FeOOH}} \cdot e^{-\frac{E_a^{\mathrm{FeOOH}}}{RT}} + A_{\mathrm{HCO_3}^-} \cdot e^{-\frac{E_a^{\mathrm{HCO_3}^-}}{RT}} a_2^n \tag{36}$$

	$CaCO_3$	$CaMg(CO_3)_2$	${HCO_3}^-$	FeOOH
Arrhenius pre-exponential factor A [1/s]	6.59 $\times 10^4$	1.05 $\times 10^4$	1.04 $\times 10^9$	1.64 $\times 10^7$
Arrhenius activation energy E_a [J/mole]	66000	103000	67000	86500

Table 8: Input for calcite, dolomite and goethite.

	$CaCO_3$	$CaMg(CO_3)_2$	FeOOH
A_1	4.764488e+003	7.592995e+003	-7.256759e+003
A_2	1.443789+000	2.356035e+000	-1.978556e+000
A_3	-1.965495e+005	-3.074160e+005	3.226989e+005
A_4	-1.855352e+003	-2.967791e+003	2.782977e+003
A_5	8.937845e+006	1.377927e+007	-1.548242e+007
A_6	-4.900053e-004	-8.182717e-004	5.886823e-004

Table 9: Parameters of K^1, K^2 and K^3 for calcite, dolomite and goethite.

pH	6.5
n	1.6

Table 10: Parameters for calcite, dolomite and goethite.

	a_1^{eq}	a_2^{eq}	a_3^{eq}	a_5^{eq}	pH
$T = 20\ ^o$C	0.007051	0.001411	3.5046e-06	6.2262e-21	6.84
$T = 80\ ^o$C	0.003963	0.0007928	4.6181e-07	9.4936e-22	6.5

Table 11: Equilibrium values of Ca^{2+}, ${HCO_3}^-$, Mg^{2+}, Fe^{3+} and pH.

In figure 5 and 6, the numerical solutions of system (30) are plotted against time for $T = 20\ ^o$C. The initial conditions are the equilibrium points of system (30) for $T = 80\ ^o$C. We have used the Forward Euler method for the approximations. In figures 5, the $y-$axis is scaled as equation (20).

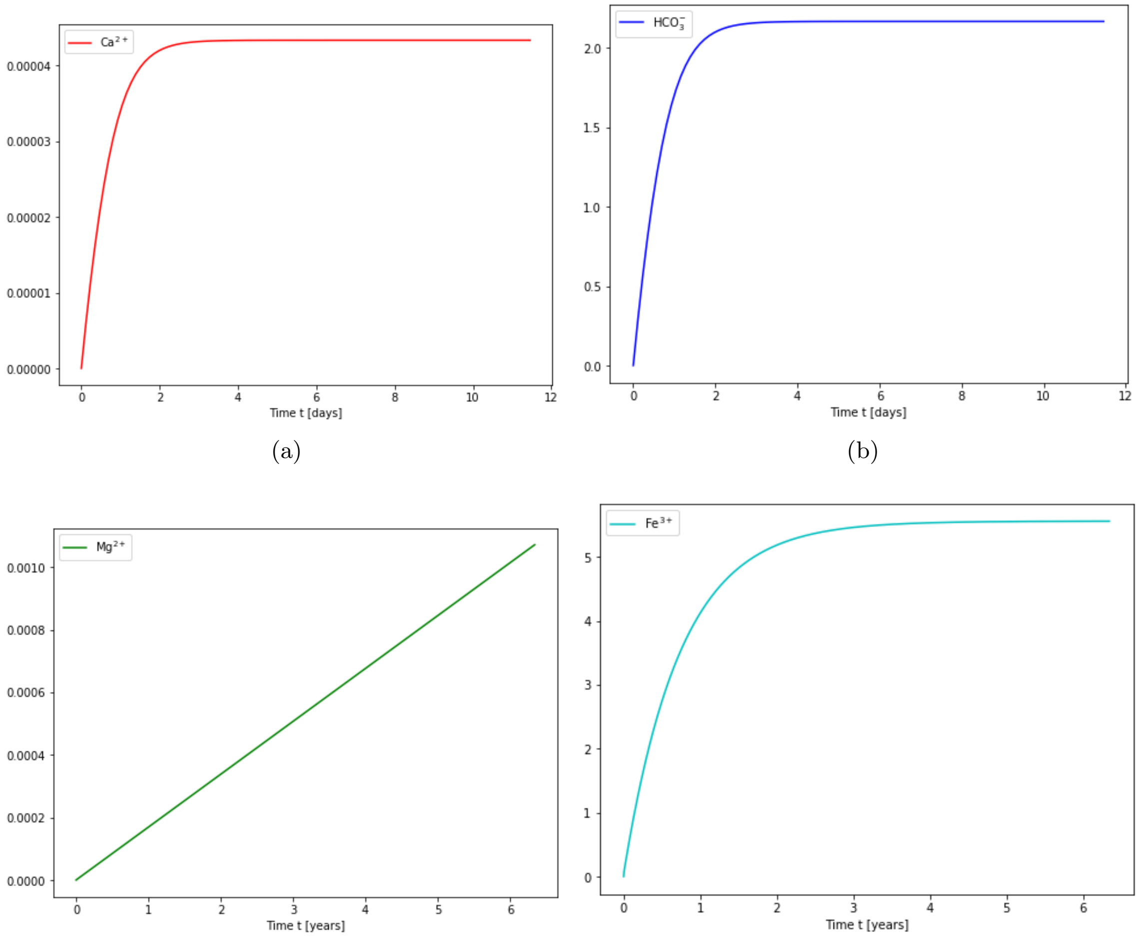

(a) (b)

(c) (d)

Figure 5: The following activities are plotted against time: (a) activity of Ca^{2+} versus time in days, (b) activity of $\mathrm{HCO_3}^-$ versus time in days, (c) activity of Mg^{2+} versus time in years, (d) activity of Fe^{2+} versus time in years. The temperature decreases from $T = 80\ ^o\mathrm{C}$ to $T = 20\ ^o\mathrm{C}$ in each graph.

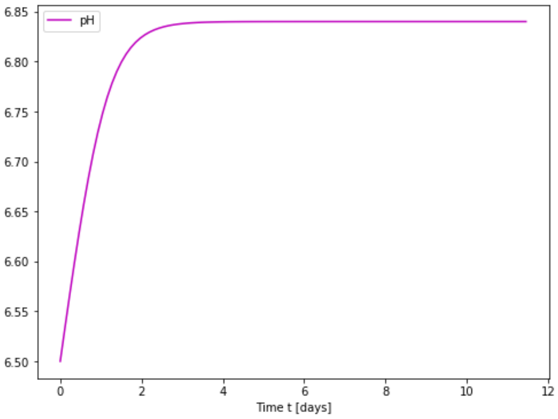

(a)

Figure 6: The pH versus time in days. The temperature decreases from $T = 80\ ^o\mathrm{C}$ to $T = 20\ ^o\mathrm{C}$.

5. Discussion

In tank 1, the temperature remains constant. So we would expect that all reactions remain in equilibrium. However, a degasser is included in tank 1. The function of the degasser is to remove gasses from the water. In our case, the dissolved gas CO_2 is removed. Due to this removal, the equilibrium of the reactions that include the ions ${HCO_3}^-$ and H^+ shifts. This is because the dissolved CO_2 reacts with water to form carbonic acid H_2CO_3, which rapidly disassociates to form the ions ${HCO_3}^-$ and H^+. So removing CO_2 triggers the reactions that depend on the ions ${HCO_3}^-$ and H^+. From the 5 mineralisation reactions that we have studied, the minerals calcite, dolomite and goethite are triggered by the degasser. Since these reactions reach equilibrium in days or years and the water remains in this tank for approximately 5 minutes, we can conclude that the minerals calcite, dolomite and goethite have no important influence in the clogging process in tank 1.

The first main temperature change happens in tank 2. Here, the temperature decreases, which means that all reactions are triggered. The water remains approximately 1 minute in this tank. So the minerals that precipitate within a short time (with order of seconds or minutes) have a influence on the clogging process in this tank. From the 5 mineralisation reactions that we have studied, only the minerals halite and barite satisfy this short-time scale. However, all the precipitated minerals are removed from the water by the filter in tank 2. So the minerals halite and barite have no influence in the clogging process in tank 2.

The water remains in tank 3 for a short time, approximately 24 minutes. So from the 5 minerals that we have studied, halite and barite have an influence on the clogging process in tank 3 since these minerals correspond to the short-time scale. However, the precipitation of halite reached its equilibrium in tank 2 and all the precipitated halite is removed from the water by the filter in tank 2. Hence, halite has no effect in the clogging process in tank 3. The mineralisation of barite still continues in tank 3 after it is triggered in tank 2. This is because it takes approximately half an hour for the reaction of barite to reach its equilibrium. Thus, only the mineralisation of barite has a significant effect on the clogging process in tank 3.

After injecting the cooled water in tank 4, the water stays there for approximately 6 years. The temperature increases in this tank. Due to this temperature increase, only the precipitations of calcite, dolomite and goethite have an impact on the clogging process in the geothermal reservoir.

6. Conclusion and outlook

In this section, we will first give a conclusion. Afterwards, we will give some recommendations for further research.

Until now, we have divided the geothermal doublet into 4 tanks and we have developed a method to determine the rate equation of a general chemical reaction. Eventually, we have used this method for 5 different mineralisation reactions. We can now determine which minerals play an important role in the clogging process in each part of the geothermal doublet. We can conclude that barite has a significant influence on the clogging process in tank 3. The minerals calcite, dolomite and goethite have an important influence on the clogging process in tank 4. None of the minerals have any significant effect on the clogging process in tank 1 and 2.

The following improvements can be made about this project:

- Adding more minerals to the research such that we can analyse which minerals are important in the clogging process.
- Include spatial dependencies in the model. This will lead to a model with partial differential equations that will describe the behaviour of the dissolved minerals.

Bibliography

- Rimstidt, J. D. (2014). Geochemical Rate Models. Cambridge, Verenigd Koninkrijk: Cambridge University Press.
- Lasaga, A. C. (2014). Kinetic Theory in the Earth Sciences. Amsterdam, Nederland: Amsterdam University Press.
- Braun, M. (1992). Differential Equations and Their Applications. New York, Verenigde Staten: Springer Publishing.
- Vuik, M. J., Vermolen, F. J., Gijzen, M. B., & Vuik, M. J. (2015). Numerical Methods for Ordinary Differential Equations. Delft, Nederland: TU Delft.